

ChemComm

Accepted Manuscript



This is an *Accepted Manuscript*, which has been through the Royal Society of Chemistry peer review process and has been accepted for publication.

Accepted Manuscripts are published online shortly after acceptance, before technical editing, formatting and proof reading. Using this free service, authors can make their results available to the community, in citable form, before we publish the edited article. We will replace this *Accepted Manuscript* with the edited and formatted *Advance Article* as soon as it is available.

You can find more information about *Accepted Manuscripts* in the [Information for Authors](#).

Please note that technical editing may introduce minor changes to the text and/or graphics, which may alter content. The journal's standard [Terms & Conditions](#) and the [Ethical guidelines](#) still apply. In no event shall the Royal Society of Chemistry be held responsible for any errors or omissions in this *Accepted Manuscript* or any consequences arising from the use of any information it contains.

Logic Gates Operated by Bipolar Photoelectrochemical Water Splitting

Received 00th January 20xx,
Accepted 00th January 20xx

G. Loget,* Gaozeng Li and Bruno Fabre*

DOI: 10.1039/x0xx00000x

www.rsc.org/

A new approach for the design of logic gates that do not involve chemical inputs is presented here. This concept is based on the polarization of a light-sensitive interface. AND and OR logic gates, working with cheap reactants, which locally triggered water splitting half reactions, were designed and operated.

The transfer of the fundamental concepts of microelectronics and integrated circuits to chemical and miniaturized fluidic systems is attracting a tremendous interest.¹⁻⁵ The design, fabrication and operation of components allowing the processing and computation of signals in these media are therefore becoming very active areas of research. There has been a growing interest on the fabrication of molecular,^{2-3,6} microfluidic,^{4,7,8} and electrochemical devices⁹⁻¹³ able to control signals or perform binary operations. In typical molecular logic gates, the operations are performed by molecules or proteins either in solution^{6,14,15} or immobilized on a surface^{3,16} that generate a detectable chemical output only in a presence of certain external input signals (e.g. optical or chemical). Besides, microfluidic-based logic operations are often based on fluids or bubbles inputs, generating optical outputs or specific patterns.⁸ Few examples of electrochemical logic gates have been reported, most of them involving redox-active molecules immobilized on an electrode and generating optical or electrical outputs.⁹⁻¹³ Other appealing examples of electrochemical Boolean operators were reported by Berggren *et al.* who used the conductivity change of a conducting polymer,¹⁷ Amatore *et al.* who designed “artificial neurons” based on paired-band microelectrode assemblies¹⁸ and Crooks *et al.* who conceived a microfluidic device generating electrochemiluminescence (ECL).¹⁹

In this context, we wish to report herein a novel approach towards logic gates operated by bipolar electrochemistry. Bipolar electrochemistry is a phenomenon that allows the generation of electrochemical reactions on the surface of conductive objects without the use of electrical wires.²⁰ It is currently attracting

considerable attention in the areas of analytical chemistry,²¹⁻²⁴ materials science,²⁵⁻³¹ motion generation³²⁻³⁵ and seawater desalination.³⁶ This phenomenon is particularly well suited for the implementation of miniaturized electrochemical systems in fluidic devices because of its inherent “wireless” nature.²⁰ So far, the unique example of logic operators based on the use of bipolar electrochemistry was reported by the group of Crooks.³⁷ Their devices were operated by electrical inputs and involved the use of ruthenium-based luminescent complexes and an amine co-reactant for the generation of ECL as an output.³⁸ The bipolar electrochemical splitting of water was reported by Fleischmann *et al.*³⁹ and applied recently for steering conducting objects^{33,34} and for the synthesis of Janus particles.⁴⁰ So far, only little interest^{41,42} has been given to the use of semiconductor (SC) bipolar electrodes (BEs). It is worth noting that Ongaro *et al.* recently reported the electric field-assisted photoreduction of metal on TiO₂ nanofibers.⁴³

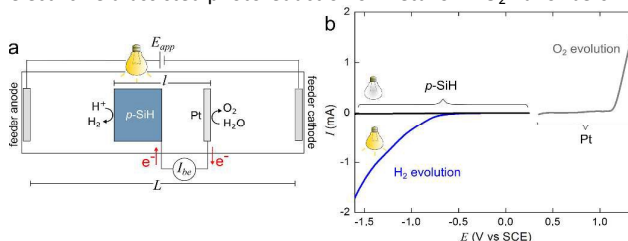


Fig 1. a) Scheme depicting the cell used for photoelectrochemical experiments performed with a *p*-SiH/Pt BE. b) Voltammetric curves showing the anodic behavior of Pt (grey) and the cathodic behavior of *p*-Si with (blue) and without (black) illumination. The curves were obtained at 50 mV·s⁻¹ in 50 mM H₂SO₄.

We introduce here a new concept for the design of bipolar photoelectrochemical logic gates using a SC surface as a reactive pole, which allows for the first time to use light as an input signal. The fabrication and operation of AND and OR logic gates are described, that operate with the bipolar photoelectrochemical splitting of water and do not require direct connections. These devices can be very easily implemented and function only with water and a low concentration of supporting electrolyte (in the mM range).

Institut des Sciences Chimiques de Rennes, UMR 6226 (MaCSE) CNRS
Université de Rennes 1, Campus de Beaulieu, 35042 Rennes Cedex, France
gabriel.loget@univ-rennes1.fr ; fabre@univ-rennes1.fr

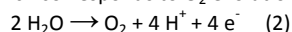
Electronic Supplementary Information (ESI) available: The experimental section, and additional data. See DOI: 10.1039/x0xx00000x

In a typical bipolar electrochemistry experiment, a conducting object is placed in an electrolytic solution between two feeder electrodes, as shown in Fig. 1a. This object can be a conductive surface (e.g. a metal wire) or junctions. The application of a potential E_{app} between the two feeder electrodes generates a potential drop in the solution and therefore leads to the generation of a polarization potential ΔV along the object surface, which is maximal between its two ends.²⁰ The value of this maximum polarization potential, ΔV_{max} , is given by the following relation:

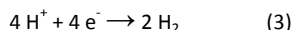
$$\Delta V_{max} = \frac{E_{app}}{L} \times l \times \theta \quad (1)$$

with L being the distance between the feeder electrodes (4.6 cm), l the characteristic length of the conducting surface and θ a dimensionless constant that depends on the potential losses of the cell.²⁹ If ΔV_{max} is sufficiently high, electrochemical reactions can be toposselectively triggered: oxidation at the anodic pole (the pole facing the feeder cathode) and reduction at the cathodic pole (the pole facing the feeder anode). The conducting surface is then behaving at the same time as an anode and a cathode, that is, a BE.²⁰ An important aspect is that electron production and consumption must be equal at both sides of the BE in order to maintain charge neutrality. In the present work, the logic gates were designed on the basis of the configuration shown in Fig. 1a, with a split-BE²⁰ composed of an oxide-free, hydrogen-terminated p -type silicon (p -SiH) cathodic pole and a Pt anodic pole, electrically connected outside to the cell. This configuration allowed to easily measure the current I_{be} flowing through the BE with an ammeter. All the reported experiments were performed in 50 mM aq H_2SO_4 in the dark and under irradiation with a halogen lamp.

First, both materials used for the split-BE were investigated separately by voltammetry in a classical three-electrode electrochemical cell. The anodic response of Pt was independent of light and, as shown in Fig. 1b, displayed an anodic current starting at 1.1 V vs SCE, which corresponds to O_2 evolution:



Unlike metals, the electrical properties of SC electrodes can be dramatically changed by light. For instance, p -type Si requires the generation of minority carriers (i.e. electrons) to operate as a photocathode, therefore irradiation with a wavelength higher than the material band gap (1.1 eV) is necessary in order to promote electrochemical reduction reactions at its surface.⁴⁴ Consistent with that, no cathodic current was generated in the dark at p -SiH (black curve in Fig. 1b) while a significant photocurrent beginning at -0.6 V vs SCE was observed under illumination (blue curve), which corresponds to proton reduction:



These preliminary data suggest that reduction of water cannot occur at the cathodic pole (p -SiH) of the BE in the dark. Because the charge consumption must be equal at both sides of the BE,²⁰ this blocking behavior should also prevent oxidation reaction to occur at the anodic pole and therefore no current should flow through the object. On the contrary, bipolar reactions should be possible under illumination, if the applied electric field is sufficiently high to generate a $\Delta V_{max} > 1.7$ V between the ends of the BE, corresponding to the thermodynamic value that must be overcome in order to trigger reactions (2) and (3), as determined by Fig. 1b.

These conditions should lead to the generation of a faradaic current I_{be} flowing through the BE, as illustrated in Fig. 1a.

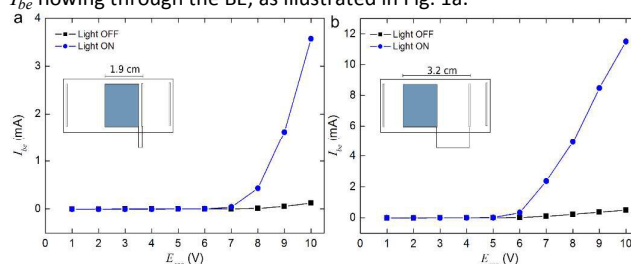


Fig. 2. Curves showing the current flowing through the BE, I_{be} as a function of the potential applied between the feeder electrodes E_{app} in the dark (black curves) and under illumination (blue curves) for a) 1.9 cm-long and b) 3.2 cm-long BE. The insets are schemes representing the corresponding cells.

In order to assess thermodynamic and kinetic parameters directly on the BE, I_{be} measurements were performed while imposing different values of E_{app} , with and without illumination. Two characteristic BE lengths, $l_1 = 1.9$ cm and $l_2 = 3.2$ cm, were used in this work. From the data shown in Fig. 2, it is obvious that a similar trend was obtained for both BEs. Under illumination, I_{be} was equal to zero until values $E_{app1} = 7$ V and $E_{app2} = 5$ V were respectively reached for l_1 and l_2 and then I_{be} increased with E_{app} . These threshold values correspond to the potentials to apply in order to generate a ΔV_{max} of 1.7 V and locally trigger reactions (2) and (3). The highest value, E_{app1} was found for the smallest l value, which is well in line with eq. (1). This relation allowed us to calculate that ~50 % of the applied electric field is effectively restituted to the BE (average $\theta = 0.54$), due to losses that may be attributed to field perturbation in the cell or potential drops at the solid/liquid or solid/solid interfaces. As expected, dark currents were found in both cases much lower than photocurrents (~25 times for $E_{app} = 10$ V, see Fig S1) thanks to the insulating behavior of p -SiH under these conditions. These data demonstrate that illumination and applied potential generate large current modifications in these BEs that can be easily measured. Therefore, such a configuration is very well-suited for the fabrication of two-input logic gates, which will be now described.

The two inputs can be defined as E_{app} ($In1$) and illumination ($In2$), whereas the current I_{be} can be considered as the output signal. Based on data of Fig. 2a, we decided to set $In1 = 0$ for $E_{app} = 7$ V and $In1 = 1$ for $E_{app} = 10$ V, in order to obtain a sufficiently high output signal when all the inputs will be equal to 1. The threshold output value was arbitrary set to 1.5 mA. The transient signals $In1$ and $In2$ and the resulting outputs for both systems are shown in Fig. 3a-c and summarized in the corresponding truth tables (Fig. 3e,f). The 1.9 cm-long BE (Fig. 3b) exhibited an output signal "1" ($I_{be} > 1.5$ mA) only when $In1 = In2 = 1$. All the other combinations yield an output signal of "0" ($I_{be} < 1.5$ mA). Therefore, this system acted as an AND gate. As shown in Fig. 3d, generation of H_2 and O_2 bubbles was observed at both reactive poles of the BE when $Output = "1"$, confirming the triggering of reactions (2) and (3). The release of H_2 bubbles from the BE surface caused the current fluctuations that are visible in the output signal. In contrast, the 3.2 cm-long BE (Fig. 3c) was found to be always in its state "1" when illuminated, which is in good agreement with the data shown in Fig. 2b. Even if the

latter configuration is not so beneficial in terms of Boolean logic (a YES gate, performing the operation $Output = In_2$), it will be very useful in the following for the design of an OR logic gate.

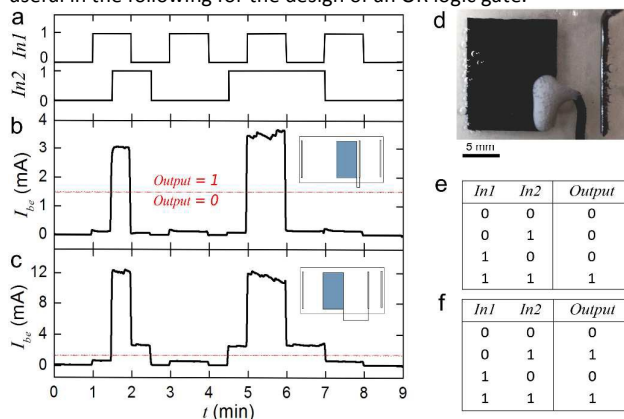


Fig. 3. Time-dependent profiles of the applied input signals a) In_1 ($In_1 = 0$ for $E_{app} = 7$ V and $In_1 = 1$ for $E_{app} = 10$ V) and In_2 ($In_2 = 0$ when the light is OFF and $In_2 = 1$ when the light is ON) and the output I_{be} measured for b) a 1.9 cm-long BE acting as an AND gate and c) a 3.2 cm-long BE. Both BEs are composed of a p -SiH cathodic pole and a Pt anodic pole. The red line indicates the threshold current of 1.5 mA. d) Photograph of the split BE showing the evolution of H_2 and O_2 bubbles at the cathodic pole (left) and at the anodic pole (right), respectively. e,f) Truth tables summarizing the results obtained in e) Fig. 3b and f) Fig. 3c.

For comparison, split BEs only composed of Pt wires were also investigated and were found to perform the following operations: $Output = "1"$ whatever the states of In_1 and In_2 for $l = 3.2$ cm (see Fig. S2 in the Supporting Information) and $Output = In_1$ for $l = 1.9$ cm, as shown in Fig. 4c. These results were expected because the conductivity of metals like Pt is not sensitive to light, therefore the output was always independent of In_2 . The latter configuration was particularly attractive since it allowed to reach the combination that was missing in the truth table of Fig. 3f in order to get an OR gate, (*i.e.* $Output = 1$ when $In_1 = 1$ and $In_2 = 0$).

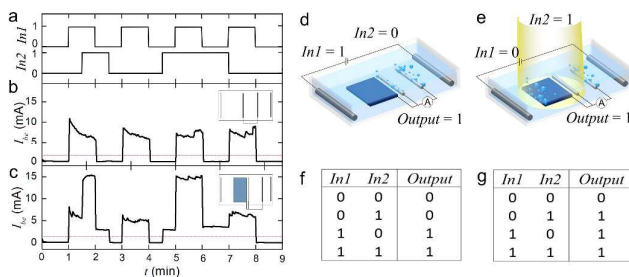


Fig. 4. Time-dependent profiles of the applied input signals a) In_1 ($In_1 = 0$ for $E_{app} = 7$ V and $In_1 = 1$ for $E_{app} = 10$ V) and In_2 ($In_2 = 0$ when the light is OFF and $In_2 = 1$ when the light is ON) and the output I_{be} measured for b) a 1.9 cm-long BE with two Pt reactive poles and c) a 3.2 cm-long BE composed of a p -SiH/Pt cathodic pole and a Pt anodic pole acting as an OR gate. The red line indicates the threshold current of 1.5 mA. d,e) Cell schemes showing the OR gate operating when f) $In_1 = 1$ and $In_2 = 0$ and g) $In_1 = 0$ and $In_2 = 1$. g,h) Truth tables summarizing the results obtained in f) Fig. 4b and g) Fig. 4c.

An interesting strategy to combine the BE configurations of Fig. 3c and 4b was to use a hybrid BE made of a light-sensitive component as well as a component non-sensitive to light. The simplest design,

depicted in Fig. 4d,e, consisted in the connection in parallel of a p -SiH surface with a Pt wire. The output signal of such a BE with the corresponding truth table are shown in Fig. 4c,g. As expected, this BE acted as an OR gate with the Pt wire being the cathodic pole when $In_1 = 1$ and $In_2 = 0$, and p -SiH being the cathodic pole when $In_1 = 0$ and $In_2 = 1$. These experiments demonstrate that AND and OR logic gates operated by bipolar photoelectrochemical water splitting can be designed and easily operated. The percentages of current flowing through the BEs were calculated for the AND and the OR logic gates and are reported in Table S1. Interestingly, they varied from values smaller than 0.4% when $Output = "0"$ to values greater than 5% when $Output = "1"$, with a maximum of 22% for the OR gate when $In_1 = In_2 = 1$. In order to assess the time stability of the involved surfaces, cycling tests were performed with the AND gate by imposing switching cycles to In_1 while keeping $In_2 = 1$. As shown in Fig. 5, I_{be} was found to be constant over numerous switching cycles. Such a stability of the p -SiH-based BE is thus very promising for future integration of the logic gates in fluidic devices.

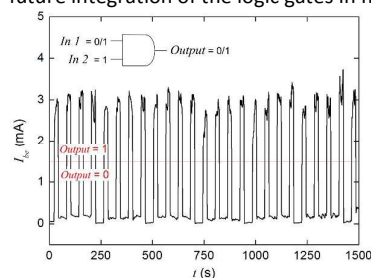


Fig. 5. Curve showing the time evolution of the output signal I_{be} for the AND gate when In_1 is switched ON and OFF. The red line indicates the threshold current 1.5 mA.

Conclusions

In this work, we have demonstrated a new strategy for the design of electrochemical logic gates working with optical and electrical inputs. Robust and stable AND and OR gates, operated with cheap reactants (*i.e.* acidic water) were fabricated. The inputs were mediated by electric and electromagnetic fields and the gates did not require direct connection. Thanks to their "wireless" implementation, these devices should be easily downscaled and therefore could be operated with LEDs in miniaturized devices such as microfluidic channels and lab-on-chips with suitable electric fields (see eq. 1). It should be also possible to combine several gates in a single fluidic device and use the current flowing through the BE to perform additional logic operations or to supply integrated electronic devices.³⁴ Additionally, a signal other than the bipolar current (*i.e.* bubble production or the generation of an optically-active compound at a reactive pole) could be considered as output, in order to minimize the electrical connections. In this first report, SC/metal BEs were employed but it is evident that our approach can be extended to p -SC/ n -SC BEs which will enlarge the panel of available operations and reduce the cost of the devices. Considering that a very large panel of materials and co-catalysts combinations can be used as BEs and that the electrolyte composition will have a direct effect on the output values, we

believe that this work pave the way to a broad family of signal processing devices for chemical and fluidic systems.

Notes and references

- 1 Y. Amir, E. Ben-Ishay, D. Levner, S. Ittah, A. Abu-Horowitz and I. Bachelet, *Nat. Nanotechnol.*, 2014, **9**, 353–357.
- 2 K. Szaciłowski, *Chem. Rev.*, 2008, **108**, 77–84.
- 3 G. De Ruiter and M. E. Van Der Boom, *Acc. Chem. Res.*, 2011, **44**, 563–573.
- 4 S. Kou, N. L. Han, D. Van Noort, K. M. K. Swamy, H. K. So, H. S. Jung, K. M. Lee, S. W. Nam, J. Yoon and S. Park, *Angew. Chem. Int. Ed.*, 2008, **47**, 872–876.
- 5 F. Meng, Y.-M. Hervault, Q. Shao, B. Hu, L. Norel, S. Rigaut and X. Chen, *Nat. Commun.*, 2014, **5**, 3023.
- 6 R. M. Zadegan, M. D. E. Jepsen, L. L. Hildebrandt, V. Birkedal and J. Kjems, *Small*, 2015, **11**, 1811–1817.
- 7 T. Thorsen, S. J. Maerkl and S. R. Quake, *Science*, 2002, **298**, 580–584.
- 8 M. Prakash and N. Gershenfeld, *Science*, 2007, **315**, 832–835.
- 9 B. Fabre, Y. Li, L. Scheres, S. P. Pujari and H. Zuilhof, *Angew. Chem. Int. Ed.*, 2013, **52**, 12024–12027.
- 10 M. Biancardo, C. Bignozzi, H. Doyle and G. Redmond, *Chem. Commun.*, 2005, **2**, 3918–3920.
- 11 L. F. O. Furtado, A. D. P. Alexiou, L. Gonçalves, H. E. Toma and K. Araki, *Angew. Chem. Int. Ed.*, 2006, **45**, 3143–3146.
- 12 S. Nitahara, T. Akiyama, S. Inoue and S. Yamada, *J. Phys. Chem. B*, 2005, **109**, 3944–3948.
- 13 K. Szaciłowski, W. Macyk and G. Stochel, *J. Am. Chem. Soc.*, 2006, **128**, 4550–4551.
- 14 B. Rout, P. Milko, M. A. Iron, L. Motiei and D. Margulies, *J. Am. Chem. Soc.*, 2013, **135**, 15330–15333.
- 15 R. Baron, O. Lioubashevski, E. Katz, T. Niazov and I. Willner, *J. Phys. Chem. A*, 2006, **110**, 8548–8553.
- 16 G. De Ruiter, E. Tartakovsky, N. Oded and M. E. Van Der Boom, *Angew. Chem. Int. Ed.*, 2010, **49**, 169–172.
- 17 D. Nilsson, N. Robinson, M. Berggren and R. Forchheimer, *Adv. Mater.*, 2005, **17**, 353–358.
- 18 C. Amatore, L. Thouin and J.-S. Warkocz, *Chem. Eur. J.*, 1999, **5**, 456–465.
- 19 W. Zhan and R. M. Crooks, *J. Am. Chem. Soc.*, 2003, **125**, 9934–9935.
- 20 S. E. Fosdick, K. N. Knust, K. Scida and R. M. Crooks, *Angew. Chem. Int. Ed.*, 2013, **52**, 10438–10456.
- 21 L. Bouffier, T. Doneux, B. Goudeau and A. Kuhn, *Anal. Chem.*, 2014, **86**, 3708–3711.
- 22 F. Zhu, J. Yan, S. Pang, Y. Zhou, B. Mao, A. Oleinick, I. Svir and C. Amatore, *Anal. Chem.*, 2014, **86**, 3138–3145.
- 23 S. E. Fosdick, S. P. Berglund, C. B. Mullins and R. M. Crooks, *Anal. Chem.*, 2013, **85**, 2493–2499.
- 24 R. K. Anand, E. Sheridan, K. N. Knust and R. M. Crooks, *Anal. Chem.*, 2011, **83**, 2351–2358.
- 25 G. Loget, D. Zigah, L. Bouffier, N. Sojic and A. Kuhn, *Acc. Chem. Res.*, 2013, **46**, 2513–2523.
- 26 J. Roche, G. Loget, D. Zigah, Z. Fattah, B. Goudeau, S. Arbault, L. Bouffier and A. Kuhn, *Chem. Sci.*, 2014, **5**, 1961–1966.
- 27 G. Loget, S. So, R. Hahn and P. Schmuki, *J. Mater. Chem. A*, 2014, **2**, 17740–17745.
- 28 G. Loget and P. Schmuki, *Langmuir*, 2014, **30**, 15356–15363.
- 29 G. Loget, J. Roche and A. Kuhn, *Adv. Mater.*, 2012, **24**, 5111–5116.
- 30 S. Ramakrishnan and C. Shannon, *Langmuir*, 2010, **26**, 4602–4606.
- 31 M. Wood and B. Zhang, *ACS Nano*, 2015, **9**, 2454–2464.
- 32 G. Loget and A. Kuhn, *J. Am. Chem. Soc.*, 2010, **132**, 15918–15919.
- 33 G. Loget and A. Kuhn, *Nat. Commun.*, 2011, **2**, 535.
- 34 J. Roche, S. Carrara, J. Sanchez, J. Lannelongue, G. Loget, L. Bouffier, P. Fischer and A. Kuhn, *Sci. Rep.*, 2014, **4**, 6705.
- 35 A. Srinivasan, J. Roche, V. Ravaine and A. Kuhn, *Soft Matter*, 2015, DOI:10.1039/C5SM00273G.
- 36 K. N. Knust, D. Hlushkou, R. K. Anand, U. Tallarek and R. M. Crooks, *Angew. Chem. Int. Ed.*, 2013, **52**, 8107–8110.
- 37 B. Y. Chang, J. a. Crooks, K. F. Chow, F. Mavré and R. M. Crooks, *J. Am. Chem. Soc.*, 2010, **132**, 15404–15409.
- 38 W. Miao, *Chem. Rev.*, 2008, **108**, 2506–2553.
- 39 M. Fleischmann, J. Ghoroghchian, D. Rolison and S. Pons, *J. Phys. Chem.*, 1986, **90**, 6392–6400.
- 40 G. Loget, J. Roche, E. Gianessi, L. Bouffier and A. Kuhn, *J. Am. Chem. Soc.*, 2012, **134**, 20033–20036.
- 41 S. Cattarin and M. M. Musiani, *J. Electrochem. Soc.*, 1995, **142**, 3786.
- 42 E. Said, N. D. Robinson, D. Nilsson, P.-O. Svensson and M. Berggren, *Electrochem. Solid-State Lett.*, 2005, **8**, H12–H16.
- 43 M. Ongaro, J. Roche, A. Kuhn and P. Ugo, *ChemElectroChem*, 2014, **1**, 2048–2051.
- 44 X. G. Zhang in *Electrochemistry of Silicon and its Oxide*, Kluwer Academic/Plenum Publishers, New York, 2001.